Genetic dissection of pheromone processing reveals main olfactory system-mediated social behaviors in mice

Tomohiko Matsuo[a], Tatsuya Hattori[b], Akari Asaba[b], Naokazu Inoue[c,d], Nobuhiro Kanomata[e], Takefumi Kikusui[b], Reiko Kobayakawa[a,1], and Ko Kobayakawa[a,f,1]

[a]Department of Functional Neuroscience, Osaka Bioscience Institute, Osaka 565-0874, Japan; [b]Companion-Animal Research, School of Veterinary Medicine, Azabu University, Kanagawa 229-8501, Japan; [c]Research Institute for Microbial Diseases, Osaka University, Osaka 565-0871, Japan; [d]Department of Cell Science, Institutes for Biomedical Sciences, School of Medicine, Fukushima Medical University, Fukushima 960-1295, Japan; [e]Department of Chemistry and Biochemistry, Waseda University, Tokyo 169-8555, Japan; and [f]Precursory Research for Embryonic Science and Technology, Japan Science and Technology Agency, Saitama 332-0012, Japan

Edited by Shigetada Nakanishi, Osaka Bioscience Institute, Suita, Japan, and approved December 11, 2014 (received for review August 29, 2014)

Most mammals have two major olfactory subsystems: the main olfactory system (MOS) and vomeronasal system (VNS). It is now widely accepted that the range of pheromones that control social behaviors are processed by both the VNS and the MOS. However, the functional contributions of each subsystem in social behavior remain unclear. To genetically dissociate the MOS and VNS functions, we established two conditional knockout mouse lines that led to either loss-of-function in the entire MOS or in the dorsal MOS. Mice with whole-MOS loss-of-function displayed severe defects in active sniffing and poor survival through the neonatal period. In contrast, when loss-of-function was confined to the dorsal MOB, sniffing behavior, pheromone recognition, and VNS activity were maintained. However, defects in a wide spectrum of social behaviors were observed: attraction to female urine and the accompanying ultrasonic vocalizations, chemoinvestigatory preference, aggression, maternal behaviors, and risk-assessment behaviors in response to an alarm pheromone. Functional dissociation of pheromone detection and pheromonal induction of behaviors showed the anterior olfactory nucleus (AON)-regulated social behaviors downstream from the MOS. Lesion analysis and neural activation mapping showed pheromonal activation in multiple amygdaloid and hypothalamic nuclei, important regions for the expression of social behavior, was dependent on MOS and AON functions. Identification of the MOS-AON–mediated pheromone pathway may provide insights into pheromone signaling in animals that do not possess a functional VNS, including humans.

social behavior | pheromone processing | main olfactory system | vomeronasal system

Most mammals have two major olfactory subsystems–the main olfactory system (MOS) and vomeronasal system (VNS). The MOS comprises the main olfactory epithelium (MOE), in which olfactory sensory neurons detect odorants, and their projection target, the main olfactory bulb (MOB) (Fig. S1*A*). Although the MOS is thought to detect volatile odorants and the VNS is thought to be important for the detection of nonvolatile pheromones, evidence shows that the MOS is also involved in pheromone detection (1–8). Surgical blocking of odorant access to the MOE, but not surgical ablation of the vomeronasal epithelium (VNE), eliminates preference to odors from the opposite sex in ferrets (9, 10). In mice, chemical ablation of the MOE impairs male and female sexual behaviors (11, 12). In these experiments in which the MOE was ablated, the function of the VNS is not directly disrupted, because the VNS is activated by direct application of urine to the nostril. Thus, these results indicate that the MOS also contributes to pheromone processing and related behaviors.

Nonconditional disruption of genes encoding signal transduction proteins that are required for activation of olfactory neurons, such as cyclic nucleotide-gated channel (*Cnga2*) or adenylyl cyclase 3, impairs several social behaviors (11, 13–15). However, complete loss of MOS function causes anosmia and severely impairs sniffing and chemoinvestigatory behaviors (11, 13, 14, 16). Chemoinvestigation and the accompanying physical contact of the nose and pheromone source are essential for VNS activation; therefore, the loss of MOS function indirectly impairs the VNS, because the VNS becomes behaviorally isolated from pheromone cues in mice (16–19).

Therefore, it is useful to establish a novel animal model, in which functions of the MOS in controlling social behavior are genetically dissociated from those of the VNS to answer several fundamental questions, such as which social behaviors are regulated by the MOS or what is the difference between the MOS and VNS in regulating social behaviors? A further question is whether the MOS has its own pheromone pathway in the brain, separate from the VNS. These questions are also important for understanding pheromone-induced social behaviors in animals that do not possess a functional VNS, such as humans.

In this study, we established two *Cnga2* conditional knockout mouse lines with regional differences in the extent of loss-of-function in the MOS: (*i*) MOS-specific conditional *Cnga2* knockout mice, the ΔMOS(cng) line, which had severe defects in active sniffing and poor survival through the neonatal period; and (*ii*) *Cnga2* conditional knockout mice with loss-of-function confined to the olfactory sensory neurons in the dorsal zone, the ΔD(cng) line. The ΔD(cng) mice and the previously generated

Significance

It is now widely accepted that the range of pheromones that control social behaviors are processed by both the vomeronasal system (VNS) and the main olfactory system (MOS). However, the functional contributions of each subsystem in social behavior remain unclear. Here, we showed that mice with loss-of-function confined to the dorsal MOS maintained innate odor recognition and VNS activity, but failed to demonstrate multiple male and female social behaviors. Functional dissociation of the MOS and VNS enabled the identification of an MOS-mediated processing of semiochemical information, independent of the VNS.

Author contributions: R.K. and K.K. designed research; T.M., T.H., A.A., N.I., N.K., T.K., R.K., and K.K. performed research; T.M., R.K., and K.K. analyzed data; and T.M., R.K., and K.K. wrote the paper.

The authors declare no conflict of interest.

This article is a PNAS Direct Submission.

Freely available online through the PNAS open access option.

[1]To whom correspondence may be addressed. Email: reiko@obi.or.jp or kobayakawa@obi.or.jp.

This article contains supporting information online at www.pnas.org/lookup/suppl/doi:10.1073/pnas.1416723112/-/DCSupplemental.

ΔD(dta) mice, in which the dorsal part of the MOB is deleted by targeted expression of the diphtheria toxin fragment-A (dta) gene (20) (Fig. 1*A* and Fig. S1*B*), maintained the ability to smell and chemoinvestigate their conspecifics. These mice therefore showed preserved pheromonal activity in the VNS, but had defects in sexual, maternal, aggressive, and risk-assessment behaviors. This functional dissection of the MOS and VNS enabled us to demonstrate social behaviors that are regulated by the MOS in a VNS-independent manner and to further characterize functional roles for the MOS-mediated pheromone pathway.

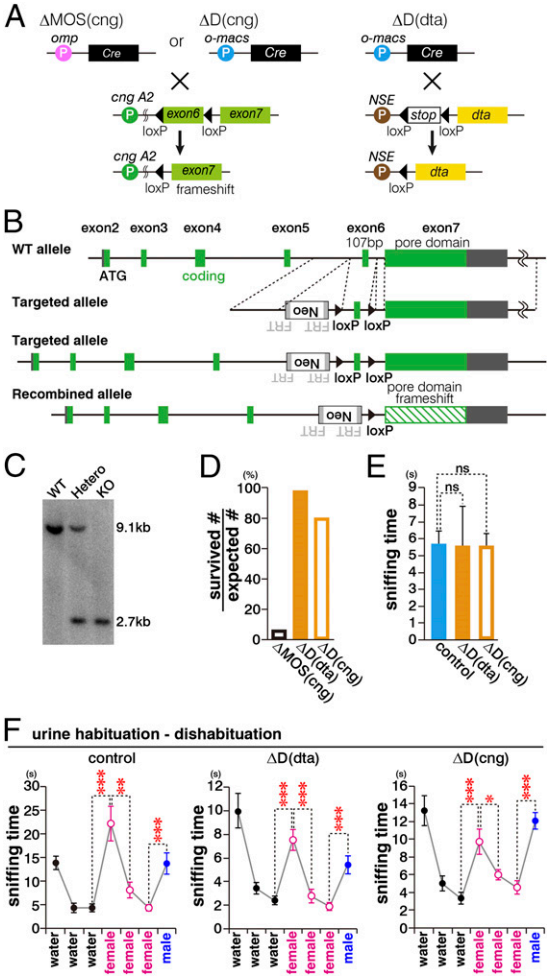

Fig. 1. Preserved detection of odors and pheromones in ΔD mice. (*A*) Strategy for generating ΔMOS(cng) mice, ΔD(dta) mice, and ΔD(cng) mice. (*B*) Schematic diagram for generating *Cnga2* conditional knockout mice. Following Cre recombination, exon 6 is deleted resulting in a frameshift of exon 7, which contains the channel pore and cAMP binding domains. (*C*) Verification of homologous recombination by Southern blot analysis. The 9.1-kb band is from the wild-type allele, and the 2.7-kb band is from the targeted allele. (*D*) Most of the ΔMOS(cng) mice die before weaning (3–4 wk old), whereas ΔD(dta) or ΔD(cng) mice do not. The number of surviving mice at the time of weaning was divided by the expected birth number to calculate survival rate. (*E*) ΔD(dta), ΔD(cng), and control mice spend similar amounts of time sniffing eugenol ($n = 6$ for each genotype). (*F*) Urine habituation-dishabituation test. Graphs present total amount of time (in seconds, s) that male control ($n = 8$), ΔD(dta) ($n = 7$), and ΔD(cng) ($n = 8$) mice spend sniffing a piece of filter paper spotted with water or urine from male or female mice. A decrease or increase in sniffing time indicates that the mice perceive the presented odor to be same as, or different from, the previously presented odor, respectively. *O-MACS*$^{cre/+}$ mice were used as controls. NSE, neuron-specific enolase, pan-neuronal promoter; dta, diphtheria toxin A. Data are presented as mean + SEM or mean ± SEM; $^{*}P < 0.05$; $^{**}P < 0.01$; $^{***}P < 0.001$; ns, $P > 0.05$ (Student's *t* test).

Results

Functional Separation of the MOS and VNS. *Cnga2* is expressed in the olfactory sensory neurons (OSNs) and brain (21, 22). *Cnga2* knockout mice have severely impaired sniffing behavior, and most of the mutant mice die within 1–2 d of birth (23). It is unknown whether these phenotypes of *Cnga2* knockout mice are caused by lack of olfaction or deficits in the brain. To distinguish between these possibilities, we generated conditional knockout mice and eliminated the *Cnga2* gene specifically in mature OSNs using *omp*-cre mice, which express Cre recombinase in mature OSNs (Fig. 1 *A–C* and Fig. S1*B*). The resultant mutant mice are named ΔMOS(cng). More than 90% of ΔMOS(cng) mice died before weaning (Fig. 1*D*). The two surviving ΔMOS(cng) mice were severely impaired in olfaction. In a food-finding test, both of the two ΔMOS(cng) mice did not find buried food within 5 min, whereas all four control mice that we examined found the food in less than 80 s (22, 52, 71, and 72 s, respectively). ΔMOS (cng) male mice also showed reduced sniff numbers toward female intruders [12 and 11 sniffs in ΔMOS(cng) mice and 54, 59, 65, and 75 sniffs in control mice during a 15-min encounter]. These phenotypes are similar to those of *Cnga2* knockout mice (13). This finding indicates that the presence of CNGA2 in OSNs is important for pup survival and sniffing behavior. Loss of CNGA2 in OSNs affected sniffing behavior, and therefore indirectly influenced pheromone detection by the VNS. Thus, even in ΔMOS(cng) mice, functional separation of the MOS from the VNS could not be achieved.

To ensure the functional dissociation of the MOS and VNS, we used two independent mouse lines, ΔD(dta) and ΔD(cng) (Fig. 1 *A–C* and Fig. S1 *C–N*). These two lines have defects in the dorsal MOB, but they are caused by two different techniques: ablation of neurons in ΔD(dta) mice and suppression of odor-evoked activity in ΔD(cng) mice. Both strains were bred onto the *O-MACS*$^{cre/+}$ background, which express Cre recombinase specifically in olfactory neurons that project to the dorsal domain of the MOB (20). In ΔD(dta) mice, the diphtheria toxin fragment-A gene is expressed Cre-dependently under control of a neuron-specific promoter. Thus, OSNs projecting to the dorsal domain of the MOB are ablated (20). ΔD(cng) mice were generated by crossing conditional *Cnga2* knockout mice with *O-MACS*$^{cre/+}$ mice. In contrast to ΔMOS(cng) mice, most of the ΔD(dta) and ΔD(cng) mice grew to adulthood (Fig. 1*D*). We first examined sniffing ability and general olfaction in ΔD(dta) and ΔD(cng) mice. Both lines sniffed a neutral odorant, eugenol, as much as control mice did (Fig. 1*E*). A food-finding test was then carried out to evaluate olfaction in ΔD mice. The time taken for the ΔD (dta) and ΔD(cng) mice to find the buried food was similar to that of control mice [*O-MACS*$^{cre/+}$ = 69.8 ± 8.9 s, $n = 13$; ΔD (dta) = 89.0 ± 28.7 s, $n = 7$, $P = 0.22$; ΔD(cng) = 73.5 ± 12.5 s, $n = 6$, $P = 0.41$; mean ± SEM], indicating that ΔD mice have normal sniffing and general olfaction ability.

Subsequently, we tested the ability of ΔD mice to distinguish male and female urine, which contain different sets of pheromones. In a habituation-dishabituation test, both ΔD(dta) and ΔD(cng) mice discriminated female urine from water and male urine from female urine (Fig. 1*F*). This result shows that ΔD mice were able to detect and discriminate pheromones.

We next investigated whether the structure or function of the VNS is altered in ΔD mice. VNE of control, ΔD(dta), and ΔD (cng) mice had a two-layer structure comprised of Gαi2- and Gα*o*-expressing neurons (Fig. 2*A*), and expressed olfactory marker protein (OMP), a marker of mature sensory neurons, in somata and dendrites in a similar manner (Fig. 2*B*). Projections of vomeronasal neurons were not impaired, as the segregation of Gαi2- and Gα*o*-expressing neurons in the accessory olfactory

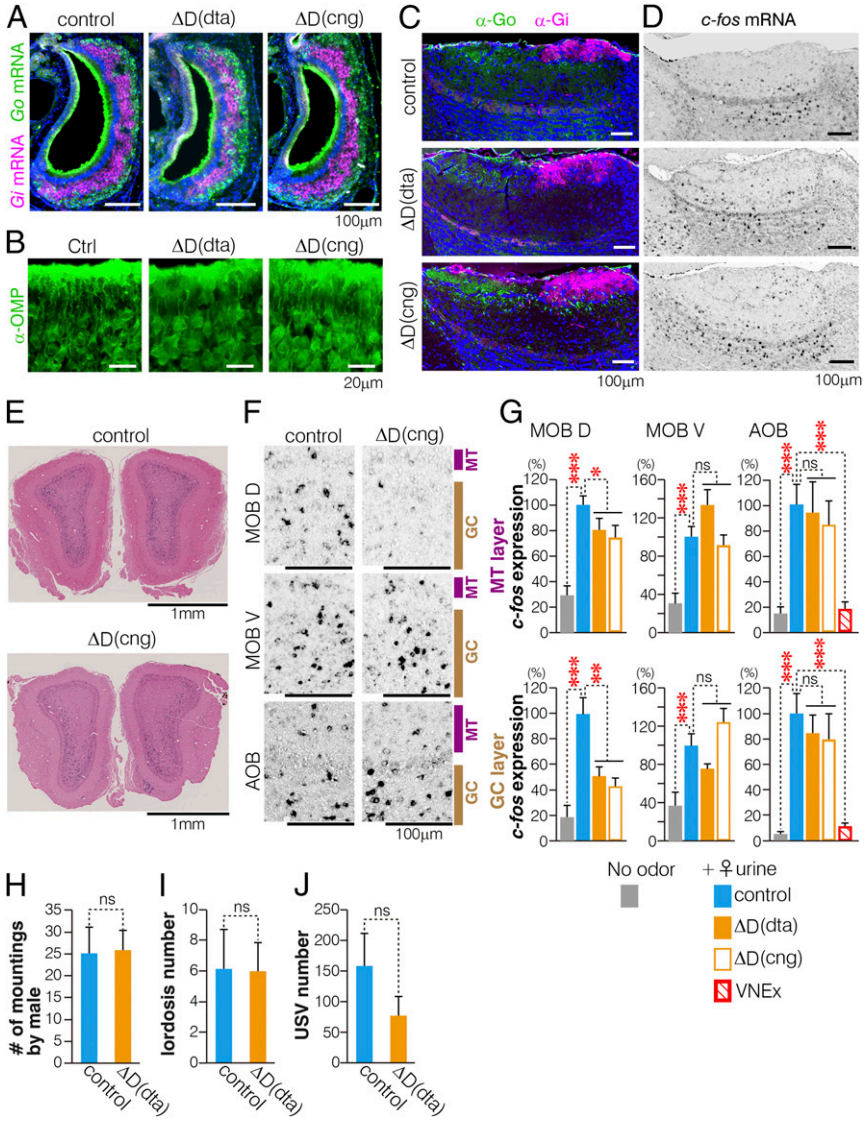

Fig. 2. Preserved VNS functions in ΔD mice. (*A* and *B*) VNE was stained with Gαi2 and Gαo riboprobes (*A*) and antibody against OMP (*B*). (*C*) Immunohistochemical images of Gαi2 and Gαo in the AOB. (*D–F*) In situ hybridization analysis of *c-fos* expression in the AOB (*D*), MOB (*E*), and magnified pictures of the dorsal (D) and ventral (V) MOB and of the AOB after exposure to female urine (*F*) (representative image). (*G*) Quantification of *c-fos* expression in the granule cell (GC) and mitral cell (MT) layers of MOB-D, MOB-V, and AOB after exposure to female urine or without odor exposure in control ($n = 8$), ΔD(dta) ($n = 6$), ΔD (cng) ($n = 8$), and VNEx ($n = 10$) mice. Values from control mice exposed to female urine have been set to 100%; other values are relative to this. (*H* and *I*) ΔD (dta) female mice show normal lordosis behavior. Control ($n = 9$) and ΔD(dta) ($n = 11$) female mice were exposed to a stud male. The numbers of mountings by male mice (*H*) and lordosis postures displayed by female mice (*I*) were measured. (*J*) Emission of USVs in response to a female intruder was not significantly changed between ΔD(dta) ($n = 5$) and control ($n = 4$) female mice. Control and ΔD(dta) female mice were exposed to a hormone-primed ovariectomized female. Control, *O-MACS*$^{cre/+}$. Data are presented as mean + SEM. $^*P < 0.05$; $^{**}P < 0.01$; $^{***}P < 0.001$; ns, $P > 0.05$ (Student's *t* test in *G–I*, and Student's *t* test and Mann–Whitney *U* test in *J*).

bulb (AOB), which is the projection target of the vomeronasal sensory neurons, was maintained in ΔD mice (Fig. 2*C* and Fig. S1*A*).

The activity of the MOS and VNS was then examined in ΔD (dta) and ΔD(cng) mice by analyzing expression of a neuronal activation marker, *c-fos*, in the MOB, the projection target of the OSNs, and AOB. *C-fos* expression increased in the mitral and granule cell layers of the dorsal and ventral MOB following exposure of male control mice to female urine (Fig. 2 *E–G*). As expected, when this was done with ΔD(dta) and ΔD(cng) mice, they showed significantly decreased *c-fos* expression compared with control mice in the granule and mitral cell layers of the dorsal domain of the MOB, to which olfactory neurons of the dorsal MOE project (Fig. 2 *E–G* and Fig. S1*A*). The expression of *c-fos* was similar to control in the ventral part of the MOB of ΔD(dta) and ΔD(cng) mice. Importantly, the AOB of ΔD(dta), ΔD(cng), and control mice showed similar expression of *c-fos* (Fig. 2 *D*, *F*, and *G*), whereas the AOB of mice with vomeronasal organ lesions (VNEx mice) had greatly reduced expression of *c-fos* (Fig. 2*G*). This finding is in contrast to mice with complete ablation of the MOE, which have been reported to show a reduction of *c-fos* expression in the AOB following exposure to estrous-female–derived odors (16, 19).

In females, the VNS is essential for lordosis (24), a receptive response that occurs during sexual behavior. Female ΔD(dta) mice were mounted by stud males and displayed lordosis postures as often as control female mice did (Fig. 2 *H* and *I*). It has been reported that female mice deficient in the VNS by surgical

ablation of the VNE or by a disruption of the *trpc2* (transient receptor potential cation channel, subfamily C, member 2) gene that encodes an ion channel essential for pheromone-evoked neural activity in vomeronasal neurons (25, 26), display male-like behaviors toward a female intruder (27); however, these behavioral abnormalities were not reproduced by surgical ablation of the VNE as reported in Martel and Baum (28). Female ΔD(dta) mice neither demonstrated mounting behavior [control = 0, $n = 4$; ΔD(dta) = 0, $n = 5$] nor emitted more ultrasonic vocalizations (USVs) than control females in response to female intruders (Fig. 2*J*). These results indicate that functions of the VNS were normal in ΔD(dta) mice with regard to neuronal activation and behavior, even though MOS activity decreased in the dorsal domain of the MOB in these mice.

Social Behavior Defects of Male ΔD Mice. Male mice show a preference for female urine over male urine (29). We tested whether this sexual preference is maintained in ΔD mice. In male ΔD (dta) and ΔD(cng) mice, investigation time for female urine decreased to that spent on male urine (Fig. 3*A*). ΔD mice detected female urine and discriminated it from male urine, but failed to show sexual preference for female urine. Female urine, but not male urine, also provokes male mice to emit USVs (30). The USVs of male mice attract females and contribute to mate choice by females (31, 32). We then examined if this female urine-induced social behavior is altered in ΔD mice. In contrast to control mice, emission of USVs in response to female urine was almost completely lost in male ΔD mice (Fig. 3*B*). This result does not mean that ΔD mice lost any ability to emit USVs. Control male mice emit more USVs in response to female conspecifics than to male conspecifics (33) (Fig. 3*C*). In ΔD mice, the number of USVs emitted in response to male conspecifics significantly increased and, as a result, they exhibited similar numbers of USVs in response to males and females (Fig. 3*C*), another example of a loss of sex-specific behavior in ΔD mice. Thus, ΔD mice did not emit USVs in a social context in which USVs would normally be emitted, but instead they emit USVs in an inappropriate social context in which USVs would normally not be emitted. These results indicate that ΔD mice cannot judge proper social contexts in which to emit USVs.

We next analyzed social behavior directed at conspecific animals. Resident mice usually investigate an intruder by sniffing intensively around the anogenital area with greater frequency than the head or body to obtain chemosensory information. The anogenital area, especially the urine, contains an abundance of pheromones and conveys social information, such as the sex or sexual receptivity, of an intruder (34). Mice with a complete loss of MOE function and chemical ablation of the MOE show a very low level of sniffing behavior toward conspecifics (13, 14). In contrast, the amount of sniffing toward male (Fig. 3*D*) and female (Fig. S2*A*) conspecifics was not reduced in ΔD(dta) and ΔD(cng) mice compared with that of control mice, indicating that ability and motivation for sniffing conspecifics is maintained in ΔD mice. However, ΔD mice did not show the anogenital preference observed in control mice (Fig. 3*E* and Fig. S2*B*). In contrast to this, VNEx mice maintained anogenital preference (29) (Fig. 3*E* and Fig. S2*B*). These results suggest that, in addition to sexual preferences, anogenital sniffing preferences are also innately controlled by the dorsal olfactory pathway.

We then asked if ΔD mice also have abnormalities in male-specific behaviors, such as aggressive and sexual behaviors. For male mice, it is important to exclude a strange male intruder from their territory through aggressive behavior. This aggressiveness of male mice can be measured by a behavioral analysis named "the resident-intruder test" (35). In this test, the fraction of mice showing aggression and the number and duration of the attacks on wild-type male intruders were significantly lower in male ΔD(dta) and ΔD(cng) mice than in control mice (Fig. 3 *F*–*H*). One possible explanation for this lack of aggression is that masculinization of

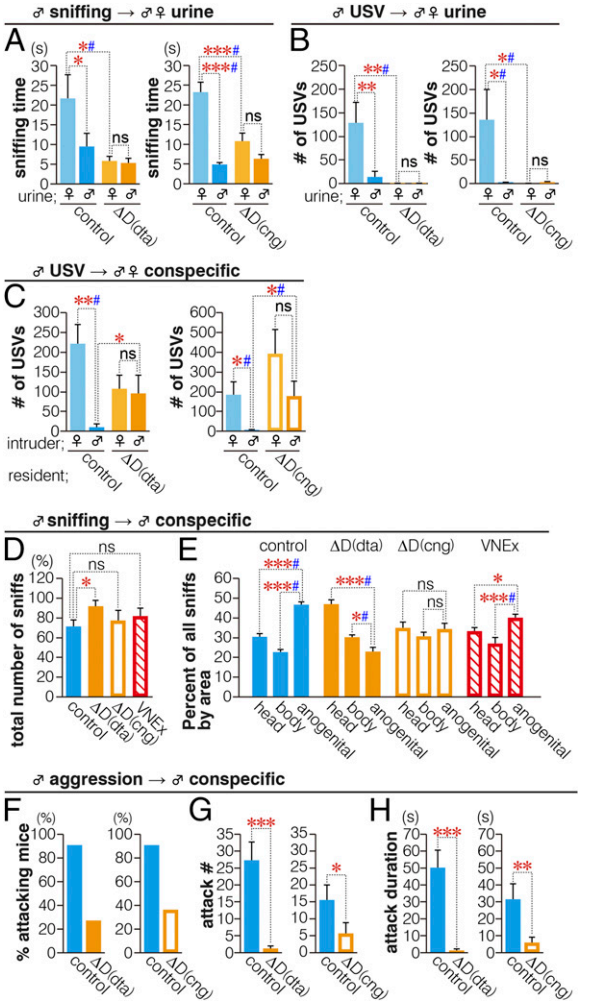

Fig. 3. Social behavior defects in male ΔD mice. (*A*) Total amount of time that male control, ΔD(dta), or ΔD(cng) mice spend sniffing male or female urine. (*Left*) Female urine, $n = 7$ for each genotype; male urine, $n = 8$ for each genotype. (*Right*) Female urine, $n = 16$ for each genotype; male urine, $n = 8$ for each genotype. (*B*) Number of USVs emitted by male control, ΔD (dta), or ΔD(cng) mice following presentation of male or female urine. (*Left*) control, female urine, $n = 22$; control, male urine, $n = 21$; ΔD(dta), female urine, $n = 24$; ΔD(dta), male urine, $n = 24$. (*Right*) $n = 10$ for each test. (*C*) Number of USVs elicited from male ΔD(dta) and ΔD(cng) mice by a wild-type male or female intruder. (*Left*) Control, female, $n = 22$; control, male, $n = 8$; ΔD(dta), female, $n = 24$; ΔD(dta), male, $n = 8$. (*Right*) $n = 10$ for each test. (*D* and *E*) Chemoinvestigatory behavior of male ΔD and VNEx mice toward a wild-type male intruder. Total number of sniffs (*D*) and the percent of all sniffs by area (*E*) were measured in a resident-intruder test. Control, $n = 26$ including *O-MACS*$^{cre/+}$ ($n = 21$) and sham-operated mice of VNE ($n = 5$); ΔD (dta), $n = 11$; ΔD(cng), $n = 11$; VNEx, $n = 11$. (*F*–*H*) Aggressive behaviors displayed by control, ΔD(dta), and ΔD(cng) resident male mice toward a male intruder. The percentages of mice that attack intruders (*F*), and the number (*G*) and duration (*H*) of attacks are shown. (*Left*) Control, $n = 11$, ΔD (dta), $n = 11$; (*Right*) control, $n = 10$, ΔD(cng), $n = 11$. *O-MACS*$^{cre/+}$ mice were used as controls unless otherwise noted. Data are presented as mean + SEM. $^{*}P < 0.05$; $^{**}P < 0.01$; $^{***}P < 0.001$; ns, $P > 0.05$ (Student's *t* test in *A*–*H*). $^{\#}P < 0.05$ (Mann–Whitney *U* test in *A*–*E*).

ΔD mice is impaired at the sex hormone level or in the brain. However, the testosterone level of ΔD(dta) mice was the same as in control mice (Fig. S2*C*), suggesting that ΔD(dta) mice possess normal male hormonal properties. We also investigated the mounting behavior of male ΔD mice toward females. In *cnga2* unconditional knockout mice, mounting behavior is completely lost (13). In contrast to this, the mounting behavior of ΔD(dta)

and ΔD(cng) mice tended to be diminished, but did not differ significantly from that of control mice (Fig. S2 *D* and *E*). This result indicates that ΔD mice have the potential to exhibit male-specific social behaviors, but they cannot link pheromonal cues to appropriate male behaviors in several social contexts.

Social Behavior Defects of Female ΔD Mice. We assumed that abnormal social behaviors in male ΔD mice were caused by alterations in sensory processing, and not by unexpected damage to brain circuits controlling male-specific behavior. If this were the case, it is possible that female ΔD mice would also exhibit abnormal social behaviors. We next investigated this possibility. Female ΔD (dta) and control mice sniffed male intruders a similar numbers of times, exhibiting a preserved ability for chemoinvestigation (Fig. 4*A*). However, anogenital preference was not observed in female ΔD(dta) mice, as in the case of male ΔD mice (Fig. 4*B*).

We next examined whether female-specific social behaviors are also altered in the ΔD mice. Pup retrieval is one such behavior, which is exhibited by even virgin females (36). Virgin female ΔD(dta) and ΔD(cng) mice had a significantly longer latency to retrieving pups compared with control mice (Fig. 4 *C* and *D*). Conversely, surgical removal of the vomeronasal organ did not have any significant effects on the latency to pup retrieval (37) (Fig. 4*E*), as reported for *Trpc2*$^{-/-}$ mice (26, 38). Nurturing the pups is an imperative behavior in female mammals that is directly linked to species preservation. It is reported that surgical ablation of the vomeronasal organ does not affect the number of pups raised (37). It is therefore interesting to examine the contribution of the MOS to the regulation of the number of pups raised. Remarkably, more than half the ΔD(dta) dams failed to raise their pups, whereas all control dams reared their pups to weaning (Fig. 4*F*). These results indicate that the MOS, but not the VNS, contributes to nurturing behaviors. The length of the estrous cycle and concentration of sex hormones in serum did not differ significantly between ΔD(dta) and control mice (Fig. 4 *G* and *H*), showing that the behavioral phenotypes observed in female ΔD(dta) were not likely to be related to altered levels of sex hormones. These findings clearly demonstrate that the MOS is required for a wide spectrum of female, as well as male social behaviors.

Altered Aversive Behaviors Induced by an Alarm Pheromone in ΔD Mice. Urine and other chemosensory cues from animals are complex sources of odorants and pheromones. Thus, the social behavior deficits observed in the ΔD mice might have been caused by changes in preference to odorant components contained in urine and produced by conspecific animals, which indirectly affected the pheromonal access to the VNS, or by the absence of functional glomeruli in the dorsal MOB, which are involved in detection of pheromones and subsequent behavioral induction. Behavioral analysis using complex cues cannot distinguish these two possibilities.

We thus next investigated whether a single pheromone is directly received by the MOS and triggers specific behaviors. SBT (2-s*ec*-butyl-4,5-dihydrothiazole) was previously isolated as a volatile pheromone present in the urine of male mice (39) that is involved in social behaviors, which was recently shown to be an active component of an alarm pheromone (40). We analyzed SBT-activated glomeruli by investigating the induction of *c-fos* expression. In control mice, SBT activated both O-MACS^{+} dorsal and O-MACS^{-} ventral glomeruli (Fig. 5 *A* and *D*). In contrast, *c-fos*$^{+}$ glomeruli were almost completely absent in the O-MACS^{+} domain of ΔD(cng) mice (Fig. 5 *B* and *E*). A few O-MACS and *c-fos* double-positive glomeruli were found close to the border of O-MACS^{+} domain of ΔD(cng) mice. These glomeruli might be innervated by olfactory neurons in which neural activity is not dependent on CNGA2 function (41, 42). In ΔD(dta) mice, O-MACS^{+} dorsal glomeruli were eliminated and

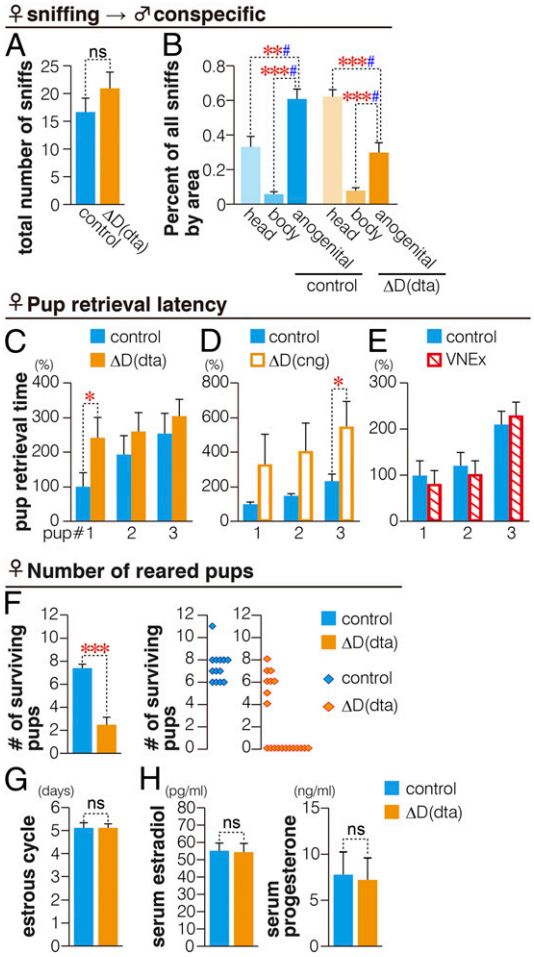

Fig. 4. Social behavior defects in female ΔD mice. (*A* and *B*) Chemoinvestigatory behavior of ΔD(dta) female mice was tested. A stud male was introduced into the female home cage. The total number of sniffs was similar between control ($n = 9$) and ΔD(dta) ($n = 11$) mice (*A*), but ΔD(dta) sniffed the head of the intruder most often (*B*). (*C–E*) Time to pup retrieval by a virgin female control ($n = 9$) vs. ΔD(dta) ($n = 9$) (*C*), control ($n = 9$) vs. ΔD(cng) ($n = 9$) (*D*), and control ($n = 11$) vs. VNEx ($n = 9$) (*E*) mice. (*F*) Average number of pups surviving to P21 when nursed by control ($n = 13$) or ΔD(dta) ($n = 20$) mothers (*Left*) and distribution of the number of surviving pups at P21 per mother (*Right*). Sixty percent of ΔD(dta) mothers (12 of 20) neglected the pups, resulting in the death of all pups. (*G*) The length of the estrous cycle did not differ between control ($n = 18$) and ΔD(dta) ($n = 11$) female mice. The estrous cycle phases were determined by vaginal smear tests. (*H*) Sex hormone levels in serum did not differ between control ($n = 8$) and ΔD(dta) ($n = 7$) female mice. *O-MACS*$^{cre/+}$ mice were used as controls in *A–D* and *F–H*. Sham-operated mice were used as controls in *E*. Data are presented as mean + SEM. $^{*}P < 0.05$; $^{**}P < 0.01$; $^{***}P < 0.001$; ns, $P > 0.05$ (Student's *t* test in *A–H*). $^{\#}P < 0.05$ (Mann–Whitney *U* test in *A* and *B*).

the remaining O-MACS^{-} domain was activated by SBT (Fig. 5 *C* and *F*). The AOB also showed weak but clear *c-fos* expression after exposure to SBT compared with the MOB (Fig. 5 *G–L*). Levels of *c-fos* expression in the AOB were similar between control and ΔD mice (Fig. 5 *M* and *N*).

Although SBT is detected by both the dorsal and ventral MOB, the detection of a pheromone does not prove that the MOS regulates social behavior triggered by that pheromone, because the MOS might detect the pheromone as a general odorant. Behavioral evidence using loss-of-function analysis in the MOS is necessary to prove this. We thus tested if ΔD mice have defects in behaviors that are triggered by SBT. ΔD(cng) mice showed increased sniffing time in response to a low

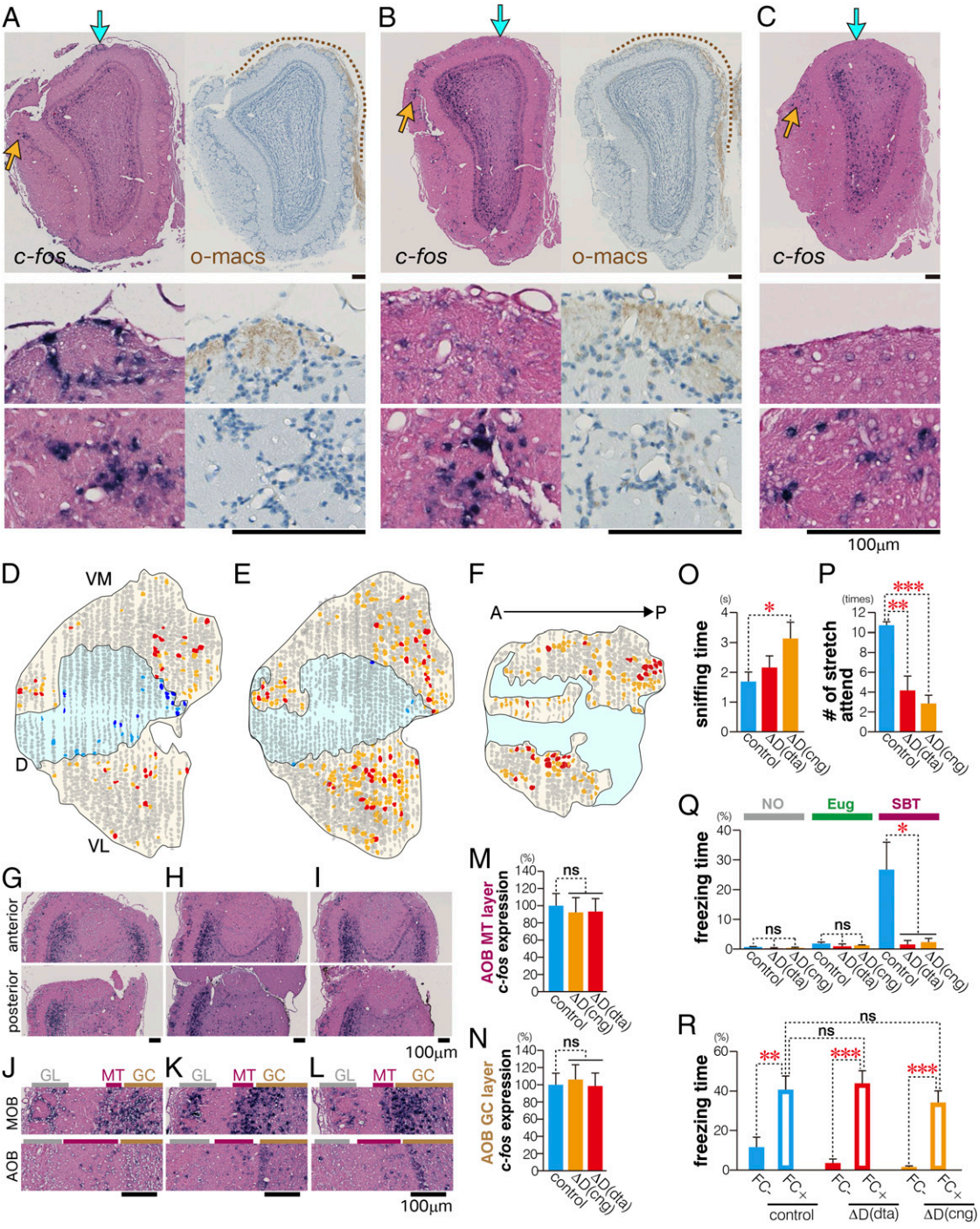

Fig. 5. Defects in SBT-triggered activation in the MOB and aversive behaviors in ΔD mice. (*A–C*) Representative images of in situ hybridization analysis of *c-fos* mRNA following exposure to SBT and immunohistochemistry of O-MACS staining in the MOB of control (*A*), ΔD(cng) (*B*), and ΔD(dta) (*C*) mice. The O-MACS$^+$ domain is indicated by a brown dot line. *Middle* and *Bottom* panels show magnified pictures of the dorsal and lateral glomeruli indicated by blue and orange arrows, respectively. An O-MACS$^+$ glomerulus of control mice (blue arrow) is surrounded by *c-fos*$^+$ periglomerular cells but not of ΔD(cng) mice in the dorsal domain. (*D–F*) Unrolled map of activated glomeruli of control (*D*), ΔD(cng) (*E*), and ΔD(dta) (*F*) mice. O-MACS$^+$ dorsal domain is colored blue. Activated glomeruli that are O-MACS$^+$ or O-MACS$^-$ are depicted in blue or red circles, respectively. Weakly activated glomeruli are pale colored (*Materials and Methods*). (*G–I*) Representative images of *c-fos* mRNA expression following exposure to SBT in the anterior (*Upper*) and posterior (*Lower*) sections of the AOB of control (*G*), ΔD(cng) (*H*), and ΔD(dta) (*I*) mice. (*J–L*) Magnified views of the MOB and AOB. *C-fos* expression was stronger in the MOB than the AOB of control (*J*), ΔD(cng) (*K*), and ΔD(dta) (*L*) mice. (*M* and *N*) Quantification of *c-fos* expression in the mitral cell (*M*) and granule cell (*N*) layers of the AOB. ($n = 4$ for each genotype) (*O*) ΔD(cng) mice show increased sniffing time on SBT compared with control mice. Sniffing time was measured during 3 min of SBT exposure [control, $n = 7$; ΔD(dta), $n = 5$; ΔD(cng), $n = 6$]. (*P*) Number of stretched attend behaviors decreased in ΔD(dta) and ΔD(cng). Stretched attend behavior was counted during 3 min of SBT exposure. (*Q*) Freezing rate of control ($n = 7$), ΔD(dta) ($n = 5$), and ΔD(cng) ($n = 6$) mice was measured after presentation of no odor, eugenol, or SBT. (*R*) ΔD(dta) and ΔD(cng) exhibit increased freezing in the presence of SBT after association of SBT with foot shock [control, $n = 13$; ΔD(dta), $n = 8$; ΔD(cng), $n = 8$]. *O-MACS*$^{cre/+}$ mice were used as controls. Data are presented as mean + SEM. *$P < 0.05$; **$P < 0.01$; ***$P < 0.001$; ns, $P > 0.05$ (Student's *t* test). A, anterior; D, dorsal; FC, fear conditioning; GC, granule cell layer; GL, glomerular layer; MT, mitral cell layer; P, posterior; VL, ventrolateral; VM, ventromedial.

concentration of SBT [the same concentration used in Brechbühl et al. (40)] compared with control mice, whereas no differences were in ΔD(dta) compared with control (Fig. 5*O*). However, both ΔD(dta) and ΔD(cng) mice showed decreased numbers of stretched attend postures, a kind of risk-assessment behavior (Fig. 5*P*), indicating that ΔD mice failed to show aversive responses to SBT. The control mice demonstrated freezing behaviors toward a high concentration of SBT; however, this behavior was not observed in the ΔD(dta) and ΔD(cng) (Fig. 5*Q*). In contrast, after conditioning an association of SBT with an electric shock, ΔD(dta) and ΔD(cng) mice showed the comparable freezing behavior in response to SBT compared with control mice (Fig. 5*R*). Because sniffing time on SBT was not reduced but rather increased in ΔD(dta) and ΔD(cng) mice, these phenotypes are not caused by indirect effects of reduced sniffing behavior, which would reduce exposure time to SBT. A previous report demonstrated that lesions in the Grueneberg ganglion (GG) reduced SBT-induced freezing and risk-assessment behavior (40). However, because *o-macs* was not expressed in the GG and OMP staining was intact in GG of ΔD(dta) mice (Fig. S3), the deficits of ΔD mice in terms of innate alarming behavior triggered by SBT were not caused by impaired GG function. Our results clearly show that the MOS contributes to the expression of freezing and aversive behaviors triggered by a single alarm pheromone, SBT. Both the MOS and GG seemed necessary for the full expression of SBT-induced behaviors.

AON Regulates Social Behavior. Our behavioral analyses using ΔMOS and ΔD mice indicated that the MOS might have dual functions for controlling social behaviors: one is an indirect function that controls sniffing to activate the VNS; the other is a direct function to control social behaviors. However, the neuronal pathways that directly control social behaviors downstream of the MOB have not been clarified. Thus, we next aimed at identifying these pathways. Male ΔD(dta) mice were able to sniff and detect female urine, but did not display the normal innate responses. Therefore, comparisons of ΔD(dta) and control mice should reveal the neuronal pathways involved in the expression of urine-induced innate behaviors, but not those that regulate sniffing and urine detection.

Secondary neurons in the MOB, termed the mitral/tufted (MT) cells, receive sensory inputs from olfactory neurons in the MOE and project to several brain areas known collectively as the olfactory cortex (43). The expression pattern of *c-fos* mRNA after exposure to estrous-female urine was examined in the following areas belonging to the olfactory cortex: anterior olfactory nucleus (AON), anterior and posterior piriform cortex (APC/PPC), olfactory tubercle (OT), and entorhinal cortex (Ent). In control mice, expression of *c-fos* mRNA was high in all of these areas except for the OT by the presentation of female urine (Fig. 6*B*), indicating that information from urine odors is processed in parallel in multiple areas of the olfactory cortex. In ΔD(dta) mice, expression of *c-fos* mRNA was comparable to that of control mice in the APC, PPC, OT, and Ent. However, the level of *c-fos* mRNA in ΔD(dta) mice was approximately half as much as in control mice in the AON only (Fig. 6 *A* and *B*). The AON maintains a rough dorsal-ventral topography of the MOB. In contrast, the topography of the MOB is lost in the piriform cortex (44) (Fig. 6*C*). This anatomical difference in the olfactory cortex might underlie the finding of decreased *c-fos* levels in the AON but not in the APC/PPC in ΔD(dta) mice. If this is the case, the dorsal AON should display reduced *c-fos* expression in response to female urine exposure, whereas the other parts of the AON should not. However, we found that ΔD(dta) mice have reduced *c-fos* expression in all parts of the AON: pars dorsalis (d), pars lateralis (l), pars ventroposterior (v), and pars medialis (m) of pars principalis (45) (Fig. 6 *D* and *E*). Expression of *arc* mRNA, an immediate-early gene often used as a marker

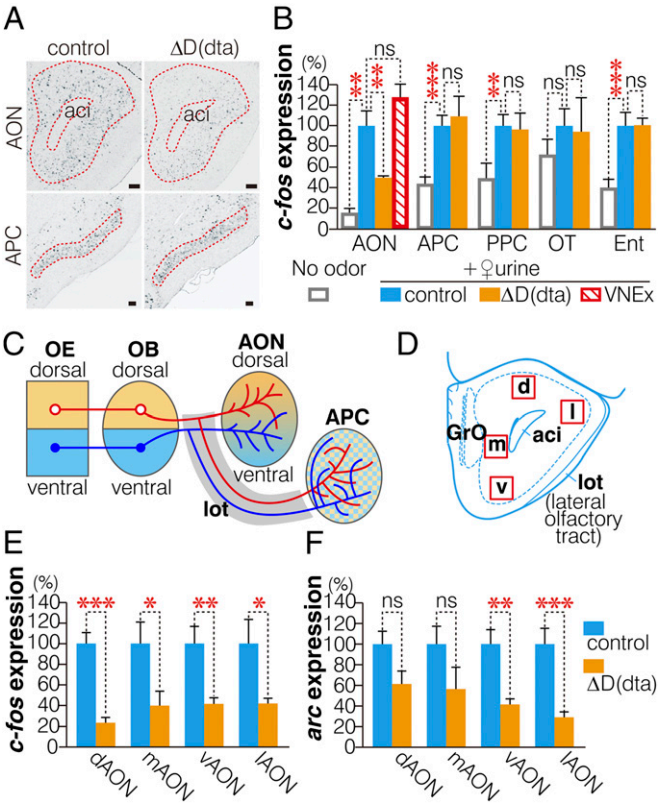

Fig. 6. Reduced *c-fos* expression in the AON of ΔD(dta) mice in response to estrous-female urine. (*A*) Representative images of in situ hybridization analysis of *c-fos* mRNA following exposure to estrous-female urine. aci, anterior commissure, intrabulbar part. (Scale bars, 100 μm.) (*B*) Levels of *c-fos* mRNA in the olfactory cortex of ΔD(dta) and VNEx mice, compared with control mice (control values set at 100%) following exposure to estrous-female urine. n = 6–10 for each *c-fos* value. (*C*) Schematic illustration showing topographic projections in the olfactory system. The AON maintains a rough dorsal-ventral topography of the MOE-MOB, whereas the APC do not. (*D*) Locations of sub regions (d, dorsal; l, lateral; v, ventral; m, medial) of the AON are illustrated. (*E* and *F*) Levels of *c-fos* and *arc* mRNA following exposure to estrous-female urine were quantified in each sub region of the AON shown in *D*. n = 8 in *E* and n = 7 in *F* for each genotype. *O-MACS*$^{cre/+}$ mice were used as controls. Data are presented as mean + SEM. $^{*}P < 0.05$; $^{**}P < 0.01$; $^{***}P < 0.001$; ns, $P > 0.05$ (Student's t test).

of neural activation, also decreased significantly in the ventral and lateral parts of the AON (Fig. 6*F*). This finding indicates that olfactory input received by the dorsal MOB is important for activation of the whole AON and that anatomical topography in the AON cannot explain the AON-specific reduction of *c-fos* expression. These data suggest that there are functional specializations among the different areas of the olfactory cortex, and that the AON controls social behaviors mediated by pheromones.

To investigate this possibility, we placed electrolytic lesions in the lateral part of the AON (Fig. S4*A*). Mice with lesions in the lateral AON (ΔAONl mice) found buried food normally and expressed levels of *c-fos* in the APC similar to those of controls (Fig. S4*B*; see also Fig. S6). The mice also sniffed intruders as often as mice that received sham operations (Fig. 7*A* and Fig. S4*C*), indicating that lateral AON lesions did not destroy olfactory sensing. However, male ΔAONl mice emitted fewer USVs in response to female urine than did sham-operated mice (Fig. 7*B*) and produced USVs even in the presence of male intruders (Fig. 7*C*). The male ΔAONl mice did not show anogenital preference during chemoinvestigation of male or female intruders (Fig. 7*D*

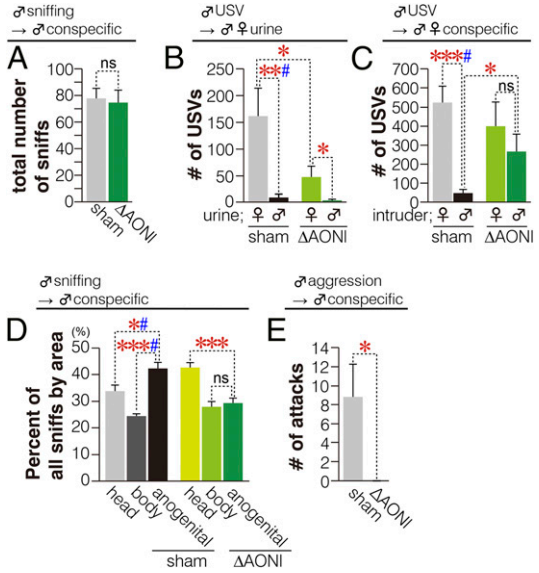

Fig. 7. Deficits in social behavior in mice with lesions of the AON. (*A*) Total number of sniffs by resident male mice that received sham operations (sham) and by resident ΔAONl male mice, toward a male intruder. (*B* and *C*) Number of USVs emitted by male sham and ΔAONl mice presented with urine-spotted paper (*B*), and in response to male or female intruders (*C*). (*D* and *E*) Resident males were exposed to male intruders. Percent of total sniffs by investigation area (*D*) and number of attacks (*E*) were measured over a 15-min period. Sham, $n = 7$; ΔAONl, $n = 8$. ΔAON, anterior-olfactory-nucleus lesioned. Data are presented as mean + SEM. $^{*}P < 0.05$; $^{**}P < 0.01$; $^{***}P < 0.001$; ns, $P > 0.05$ (Student's *t* test in *A*–*E*). $^{\#}P < 0.05$ (Mann–Whitney *U* test in *A*–*D*).

and Fig. S4*D*). Furthermore, male ΔAONl mice showed a significant reduction in aggressive behavior directed toward male mice (Fig. 7*E*). To minimize the damage to the lateral olfactory tract (lot), along which MT cells project their axons caudally (Fig. 6 *C* and *D*), we also lesioned the dorsal part of the AON (ΔAONd) and perturbed AON activity by a pharmacogenetic method using Gi-coupled designer receptors exclusively activated by the designer drug (DREADD) (46). We observed social behavior defects in both of these experiments (Figs. S4 *E*–*H* and S5). These results show that the AON is involved in the regulation of social behaviors.

The AON receives strong input from the MOB, but not from the AOB (43). Consistent with this finding, the levels of *c-fos* did not decrease in the AON of VNEx mice after exposure to female urine (Fig. 6*B*). It is highly likely that the AON is a direct downstream target of the MOB and regulates social behaviors in parallel with the VNS-mediated pheromone pathway.

Convergence of the MOS and VNS Pathways. Some social behavior defects found in ΔD mice were also reported in mice that do not have VNS functions: loss of USVs in response to female urine and decreased aggression (25–27, 47). This finding indicates that the MOS- and VNS-mediated pheromone pathways converge and integrate in yet-undefined areas in the brain. The VNS sends sensory information to multiple nuclei in the amygdala and hypothalamus (16, 48, 49). We investigated whether these areas also receive inputs from the MOS. In the amygdala of ΔD(dta) mice, expression of *c-fos* in response to estrous-female urine was significantly reduced relative to control in the following amygdaloid nuclei (Fig. 8 *A* and *C*): the posterodorsal and posteroventral regions of the medial amygdala (MePD, MePV) and the medial posterior region of the bed nucleus of the stria terminalis (BNSTMP). Expression of *c-fos* was also reduced in the medial preoptic area (MPA) of the hypothalamus of ΔD(dta) mice (Fig. 8 *B* and *D*). These four regions were also activated in a VNS-dependent manner (Fig. 8 *C* and *D*) (VNEx), indicating that sensory signals from the two olfactory subsystems converge on these regions and are essential for full activation.

In ΔD(dta) and VNEx mice, the paraventricular nuclei in the hypothalamus (PVN), which regulate sexual behaviors and olfaction-induced noncontact penile erection (50), expressed lower levels of *c-fos* than did control mice (Fig. 8 *B* and *D*). In the cortical amygdala, *c-fos* was reduced in the posterolateral nuclei (PLCo) in ΔD(dta) mice, but not in VNEx mice. In contrast, in the posteromedial nuclei (PMCo), *c-fos* was reduced in VNEx mice, but not in ΔD(dta) mice (Fig. 8*C*), consistent with findings from anatomical studies showing that the PLCo and PMCo receive direct inputs from the MOB and AOB, respectively (51).

In both ΔAONl and ΔAONd mice, *c-fos* expression was reduced in the MePD, MePV, BNSTMP, MPA, and PVN compared with control mice, but not in the PLCo (Fig. 8 *C* and *D* and Fig. S6). These observations indicate that the MOS–AON system regulates activation of amygdala and hypothalamus induced by social pheromones, which may contribute to the regulation of social behaviors (Fig. 8*E*).

Discussion

Loss-of-function analysis in the MOS has been previously carried out using several conventional techniques, such as chemical ablation of the MOE or nonconditional knockout of genes that are required for odor-evoked activation of olfactory neurons. In this

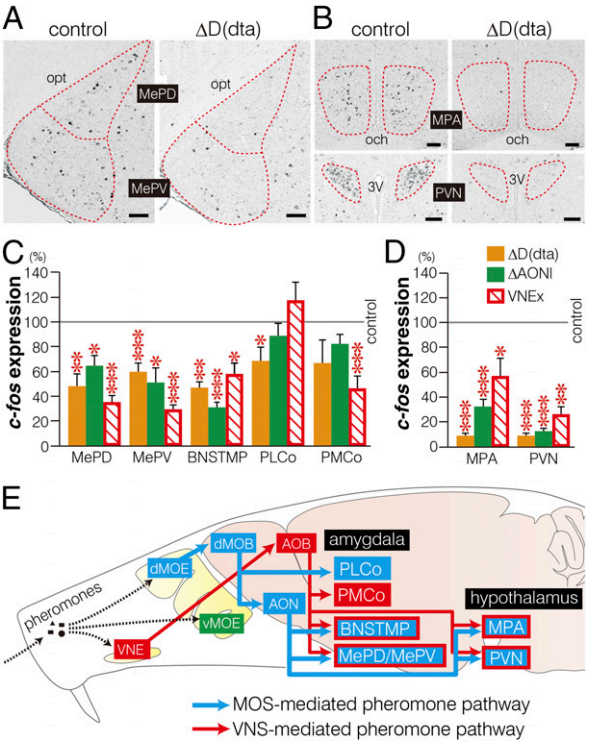

Fig. 8. Induction of *c-fos* expression in higher brain centers in response to estrous-female urine requires the MOS and AON. (*A* and *B*) Representative images of in situ hybridization for *c-fos* mRNA in the MePD, MePV (*A*), MPA, and PVN (*B*) of male control and ΔD(dta) mice exposed to urine from estrous mice. opt, optic tract; och, optic chiasm; 3V, third ventricle. (Scale bars, 100 μm.) (*C* and *D*) Percentage of *c-fos* induction, compared with control mice (horizontal line) in the amygdaloid (*C*) and hypothalamic nuclei (*D*) of ΔD(dta), ΔAONl, and VNEx mice following exposure to estrous-female urine. $n = 6$–10 for each *c-fos* value. (*E*) Model of MOS- (blue) and VNS- (red) mediated pheromone pathways in mice. The areas receiving input from both subsystems are colored both red and blue. *O-MACS*$^{cre/+}$ mice were used as controls. Data are presented as mean + SEM. $^{*}P < 0.05$; $^{**}P < 0.01$; $^{***}P < 0.001$ (Student's *t* test).

study, we generated two conditional mutant mouse strains, ΔD(dta) and ΔD(cng), which have partial defects in the MOS. This approach has a number of distinct advantages. First, these mice do not have general defects in olfaction. Second, in contrast to conventional animal models that have deficits in the MOS, they sniff and approach conspecifics no differently than do control mice, which is a prerequisite behavior for VNS activation and social behavior. Third, *c-fos* expression analysis shows that the AOB of these mice was activated normally by exposure to female urine, whereas the dorsal MOB had reduced activity. Thus, these mutant mice represent a superior animal model for dissecting functions of the MOS and VNS. The deficits shown by the ΔD(dta) and ΔD(cng) mice in multiple social behaviors indicate that the MOS has VNS-independent functions in regulating social behaviors.

Previous reports have shown that body odors from mice, which have different sets of MHC, induce different patterns of activation in the MOB (8), and some pheromones are detected by glomeruli located in the ventral domain of the MOB (2, 6, 7). The medial amygdala, which plays crucial roles in regulating social behaviors, receives more projections from the MT cells located in the ventral rather than the dorsal domain of the MOB (52, 53). These results suggest that the MOB, especially the ventral MOB, may regulate social behaviors in mouse. In this report, we show that SBT activates glomeruli located in both the dorsal and ventral MOB. The ΔD mice were defective in risk assessment and freezing behaviors induced by SBT, indicating that activation of the ventral glomeruli was not sufficient to cause SBT-induced pheromonal behaviors. These findings emphasize the importance of generating animal models that have defects in behavioral responses, like ΔD(dta) and ΔD(cng) mice, to reveal causal links between glomerular activation and behavior.

Our conclusion that the MOS is involved in multiple social behaviors is consistent with our finding that sensory input from the MOS is necessary for the activation of several amygdaloid and hypothalamic nuclei in the VNS pathway during exposure of male mice to female urine. For example, in male mice, the MPA regulates USV in response to female urine (54), and both ΔD and VNEx mice had significant reductions in expression of *c-fos* in the MPA. Moreover, the emission of USVs in response to female urine is severely reduced in ΔD and VNEx mice (47). Both subsystems are also necessary for male–male aggression (25–27). In these cases, pheromone cues are probably detected independently in the two distinct subsystems and conveyed in parallel to central brain regions, where the two signals converge to induce specific social behaviors. Anatomical analysis demonstrating that both the MOS and VNS have connections to the MPA supports this idea (1, 3). On the other hand, some social behaviors are regulated by only one of these systems: lordosis by the VNS and anogenital preference and nurturing behavior by the MOS.

Sensory input received by the MOE is conveyed to the MOB, and then to the several brain regions known as the olfactory cortex. Little is known about whether each area in the olfactory cortex has distinct functions in the processing of olfactory information. We are especially ignorant of the mechanisms and particular areas of the olfactory cortex that process pheromone signals downstream from the MOB. Because even pure pheromone molecules can activate the areas of the olfactory cortex involved in odor detection/discrimination mechanisms, it has been a challenge to distinguish whether cells activated by pheromone exposure regulate social behaviors or general odor perception.

Therefore, the behavioral dissociation found in ΔD mice (i.e., abnormal social behaviors combined with normal detection/discrimination abilities) is advantageous for identifying brain regions that regulate social behaviors, but are not related to odor detection or discrimination. In the olfactory cortex, expression of *c-fos* was reduced in the AON, but not in the APC, PPC, OT, or Ent. Lesions in the AON reproduced most of the phenotypes found in ΔD mice: namely, social behavior defects and reduced expression of *c-fos* in the amygdala and hypothalamus (MePD, MePV, BNSTMP, MPA, and PVN). Collectively, our results constitute the functional identification of pheromone circuits in the MOS; the AON receives the pheromone signals detected in the dorsal MOB, and then conveys them to central brain areas that regulate social behavior, where they converge with signals from the VNS.

Humans do not have a functional VNS, yet several odor-induced physiological responses and concurrent hypothalamic activations have been reported (55–59). Humans do have an MOS and an AON; the MOS-AON pathway identified in this study could provide new information about the neural basis of pheromone signal processing in animals without a VNS.

Materials and Methods

Construction of *Cnga2*-Floxed Mice. The *Cnga2*-floxed mice were generated by targeting exon 6 for excision by Cre recombinase. Upon verification of homologous recombination, targeted 129-derived EGR-05 embryonic stem cells were injected into C57BL/6 blastocysts, and the chimeric mice were crossed to C57BL/6 mice for at least seven generations.

Behavioral Analysis. For sniffing analysis, mice were presented three times with a filter paper spotted with distilled water; then urine from female or male mice, or eugenol, was presented. Investigation times for eugenol or urine and the third distilled water presentation were measured and subtracted to calculate the sniffing time. USVs were recorded for 5 min using a microphone (CM16/CMPA, Avisoft Bioacoustics) connected to an amplifier (UltraSoundGate 116H, Avisoft Bioacoustics), and analyzed using SAS-Lab Pro software (Avisoft Bioacoustics). For the resident-intruder test, male mice were single-housed for at least 3 wk before the test, and group-housed male 129X1/Sv mice were used as intruders. The intruder was placed in the home cage of the resident and their behavior was videotaped for 15 min. The numbers of chemoinvestigations directed at the intruder's head, body, and anogenital area, and the number and duration of aggressive behaviors, were scored. For the pup retrieval test, postnatal day (P)3 wild-type foster pups were placed in each of three corners of the home cage of individually housed virgin female mice. The times to retrieval of the first, second, and third pup were measured. To analyze nursing behavior, female mice were single-housed and mated with wild-type C57BL/6 male mice. Each morning the vaginal plug was examined; once evidence of pregnancy was visible, the male was removed. Pups that were still alive at P21 were counted. A detailed description of materials and methods is provided in *SI Materials and Methods*.

ACKNOWLEDGMENTS. We thank K. Mori for critical comments on the manuscript; N. Ogawa, S. Komaki, and T. Hasegawa for synthesizing the SBT; T. Kitsukawa for the *c-fos* plasmid; and A. Teratani, T. Iida, S. Kobayashi, A. Fukuda, K. Kawata, and Y. Esaki for technical assistance. This work was supported by the Precursory Research for Embryonic Science and Technology program of the Japan Science and Technology Agency; the Strategic Research Program for Brain Sciences of the Ministry of Education, Culture, Sports, Science, and Technology (MEXT) of Japan; the Program for Promotion of Basic and Applied Research for Innovations in Bio-oriented Industry; Japan Society for the Promotion of Science KAKENHI Grant 25750402; and the Takeda Science Foundation.

1. Boehm U, Zou Z, Buck LB (2005) Feedback loops link odor and pheromone signaling with reproduction. *Cell* 123(4):683–695.
2. Lin DY, Zhang SZ, Block E, Katz LC (2005) Encoding social signals in the mouse main olfactory bulb. *Nature* 434(7032):470–477.
3. Yoon H, Enquist LW, Dulac C (2005) Olfactory inputs to hypothalamic neurons controlling reproduction and fertility. *Cell* 123(4):669–682.
4. Spehr M, et al. (2006) Essential role of the main olfactory system in social recognition of major histocompatibility complex peptide ligands. *J Neurosci* 26(7):1961–1970.
5. Yoshikawa K, Nakagawa H, Mori N, Watanabe H, Touhara K (2013) An unsaturated aliphatic alcohol as a natural ligand for a mouse odorant receptor. *Nat Chem Biol* 9(3):160–162.
6. Lin W, Margolskee R, Donnert G, Hell SW, Restrepo D (2007) Olfactory neurons expressing transient receptor potential channel M5 (TRPM5) are involved in sensing semiochemicals. *Proc Natl Acad Sci USA* 104(7):2471–2476.
7. López F, Delgado R, López R, Bacigalupo J, Restrepo D (2014) Transduction for pheromones in the main olfactory epithelium is mediated by the Ca2+ -activated channel TRPM5. *J Neurosci* 34(9):3268–3278.

8. Schaefer ML, Young DA, Restrepo D (2001) Olfactory fingerprints for major histocompatibility complex-determined body odors. *J Neurosci* 21(7):2481–2487.
9. Kelliher KR, Baum MJ (2001) Nares occlusion eliminates heterosexual partner selection without disrupting coitus in ferrets of both sexes. *J Neurosci* 21(15):5832–5840.
10. Woodley SK, Cloe AL, Waters P, Baum MJ (2004) Effects of vomeronasal organ removal on olfactory sex discrimination and odor preferences of female ferrets. *Chem Senses* 29(8):659–669.
11. Keller M, Douhard Q, Baum MJ, Bakker J (2006) Sexual experience does not compensate for the disruptive effects of zinc sulfate—Lesioning of the main olfactory epithelium on sexual behavior in male mice. *Chem Senses* 31(8):753–762.
12. Keller M, Douhard Q, Baum MJ, Bakker J (2006) Destruction of the main olfactory epithelium reduces female sexual behavior and olfactory investigation in female mice. *Chem Senses* 31(4):315–323.
13. Mandiyan VS, Coats JK, Shah NM (2005) Deficits in sexual and aggressive behaviors in *Cnga2* mutant mice. *Nat Neurosci* 8(12):1660–1662.
14. Wang Z, et al. (2006) Pheromone detection in male mice depends on signaling through the type 3 adenylyl cyclase in the main olfactory epithelium. *J Neurosci* 26(28):7375–7379.
15. Wang Z, Storm DR (2011) Maternal behavior is impaired in female mice lacking type 3 adenylyl cyclase. *Neuropsychopharmacology* 36(4):772–781.
16. Dhungel S, Masaoka M, Rai D, Kondo Y, Sakuma Y (2011) Both olfactory epithelial and vomeronasal inputs are essential for activation of the medial amygdala and preoptic neurons of male rats. *Neuroscience* 199:225–234.
17. Keverne EB (2004) Importance of olfactory and vomeronasal systems for male sexual function. *Physiol Behav* 83(2):177–187.
18. Luo M, Fee MS, Katz LC (2003) Encoding pheromonal signals in the accessory olfactory bulb of behaving mice. *Science* 299(5610):1196–1201.
19. Martel KL, Baum MJ (2007) Sexually dimorphic activation of the accessory, but not the main, olfactory bulb in mice by urinary volatiles. *Eur J Neurosci* 26(2):463–475.
20. Kobayakawa K, et al. (2007) Innate versus learned odour processing in the mouse olfactory bulb. *Nature* 450(7169):503–508.
21. Berghard A, Buck LB, Liman ER (1996) Evidence for distinct signaling mechanisms in two mammalian olfactory sense organs. *Proc Natl Acad Sci USA* 93(6):2365–2369.
22. Kingston PA, Zufall F, Barnstable CJ (1999) Widespread expression of olfactory cyclic nucleotide-gated channel genes in rat brain: Implications for neuronal signalling. *Synapse* 32(1):1–12.
23. Brunet LJ, Gold GH, Ngai J (1996) General anosmia caused by a targeted disruption of the mouse olfactory cyclic nucleotide-gated cation channel. *Neuron* 17(4):681–693.
24. Keller M, Pierman S, Douhard Q, Baum MJ, Bakker J (2006) The vomeronasal organ is required for the expression of lordosis behaviour, but not sex discrimination in female mice. *Eur J Neurosci* 23(2):521–530.
25. Leypold BG, et al. (2002) Altered sexual and social behaviors in *trp2* mutant mice. *Proc Natl Acad Sci USA* 99(9):6376–6381.
26. Stowers L, Holy TE, Meister M, Dulac C, Koentges G (2002) Loss of sex discrimination and male-male aggression in mice deficient for TRP2. *Science* 295(5559):1493–1500.
27. Kimchi T, Xu J, Dulac C (2007) A functional circuit underlying male sexual behaviour in the female mouse brain. *Nature* 448(7157):1009–1014.
28. Martel KL, Baum MJ (2009) Adult testosterone treatment but not surgical disruption of vomeronasal function augments male-typical sexual behavior in female mice. *J Neurosci* 29(24):7658–7666.
29. Pankevich DE, Baum MJ, Cherry JA (2004) Olfactory sex discrimination persists, whereas the preference for urinary odorants from estrous females disappears in male mice after vomeronasal organ removal. *J Neurosci* 24(42):9451–9457.
30. Nyby J, Wysocki CJ, Whitney G, Dizinno G (1977) Pheromonal regulation of male mouse ultrasonic courtship (*Mus musculus*). *Anim Behav* 25(2):333–341.
31. Asaba A, et al. (2014) Developmental social environment imprints female preference for male song in mice. *PLoS ONE* 9(2):e87186.
32. Hammerschmidt K, Radyushkin K, Ehrenreich H, Fischer J (2009) Female mice respond to male ultrasonic 'songs' with approach behaviour. *Biol Lett* 5(5):589–592.
33. Whitney G, Coble JR, Stockton MD, Tilson EF (1973) Ultrasonic emissions: Do they facilitate courtship of mice. *J Comp Physiol Psychol* 84(3):445–452.
34. Wyatt TD (2003) *Pheromones and Animal Behaviour: Communication by Smell and Taste* (Cambridge Univ Press, New York), p xv.
35. Kikusui T (2013) Analysis of male aggressive and sexual behavior in mice. *Methods Mol Biol* 1068:307–318.
36. Noirot E (1969) Serial order of maternal responses in mice. *Anim Behav* 17(3):547–550.
37. Lepri JJ, Wysocki CJ, Vandenbergh JG (1985) Mouse vomeronasal organ: Effects on chemosignal production and maternal behavior. *Physiol Behav* 35(5):809–814.
38. Fraser EJ, Shah NM (2014) Complex chemosensory control of female reproductive behaviors. *PLoS ONE* 9(2):e90368.
39. Novotny M, Harvey S, Jemiolo B, Alberts J (1985) Synthetic pheromones that promote inter-male aggression in mice. *Proc Natl Acad Sci USA* 82(7):2059–2061.
40. Brechbühl J, et al. (2013) Mouse alarm pheromone shares structural similarity with predator scents. *Proc Natl Acad Sci USA* 110(12):4762–4767.
41. Bepari AK, Watanabe K, Yamaguchi M, Tamamaki N, Takebayashi H (2012) Visualization of odor-induced neuronal activity by immediate early gene expression. *BMC Neurosci* 13:140.
42. Lin W, Arellano J, Slotnick B, Restrepo D (2004) Odors detected by mice deficient in cyclic nucleotide-gated channel subunit A2 stimulate the main olfactory system. *J Neurosci* 24(14):3703–3710.
43. Paxinos G (2004) *The Rat Nervous System* (Elsevier Academic, London), 3rd Ed, xvii.
44. Miyamichi K, et al. (2011) Cortical representations of olfactory input by trans-synaptic tracing. *Nature* 472(7342):191–196.
45. Brunjes PC, Illig KR, Meyer EA (2005) A field guide to the anterior olfactory nucleus (cortex). *Brain Res Brain Res Rev* 50(2):305–335.
46. Armbruster BN, Li X, Pausch MH, Herlitze S, Roth BL (2007) Evolving the lock to fit the key to create a family of G protein-coupled receptors potently activated by an inert ligand. *Proc Natl Acad Sci USA* 104(12):5163–5168.
47. Wysocki CJ, Nyby J, Whitney G, Beauchamp GK, Katz Y (1982) The vomeronasal organ: Primary role in mouse chemosensory gender recognition. *Physiol Behav* 29(2): 315–327.
48. Samuelsen CL, Meredith M (2009) The vomeronasal organ is required for the male mouse medial amygdala response to chemical-communication signals, as assessed by immediate early gene expression. *Neuroscience* 164(4):1468–1476.
49. Meredith M (1998) Vomeronasal, olfactory, hormonal convergence in the brain. Cooperation or coincidence? *Ann N Y Acad Sci* 855:349–361.
50. Argiolas A, Melis MR (2005) Central control of penile erection: Role of the paraventricular nucleus of the hypothalamus. *Prog Neurobiol* 76(1):1–21.
51. Pro-Sistiaga P, et al. (2007) Convergence of olfactory and vomeronasal projections in the rat basal telencephalon. *J Comp Neurol* 504(4):346–362.
52. Kang N, Baum MJ, Cherry JA (2009) A direct main olfactory bulb projection to the 'vomeronasal' amygdala in female mice selectively responds to volatile pheromones from males. *Eur J Neurosci* 29(3):624–634.
53. Thompson JA, Salcedo E, Restrepo D, Finger TE (2012) Second-order input to the medial amygdala from olfactory sensory neurons expressing the transduction channel TRPM5. *J Comp Neurol* 520(8):1819–1830.
54. Matochik JA, Sipos ML, Nyby JG, Barfield RJ (1994) Intracranial androgenic activation of male-typical behaviors in house mice: Motivation versus performance. *Behav Brain Res* 60(2):141–149.
55. Savic I, Berglund H, Gulyas B, Roland P (2001) Smelling of odorous sex hormone-like compounds causes sex-differentiated hypothalamic activations in humans. *Neuron* 31(4):661–668.
56. Burke SM, Veltman DJ, Gerber J, Hummel T, Bakker J (2012) Heterosexual men and women both show a hypothalamic response to the chemo-signal androstadienone. *PLoS ONE* 7(7):e40993.
57. Stern K, McClintock MK (1998) Regulation of ovulation by human pheromones. *Nature* 392(6672):177–179.
58. Jacob S, McClintock MK (2000) Psychological state and mood effects of steroidal chemosignals in women and men. *Horm Behav* 37(1):57–78.
59. Wyart C, et al. (2007) Smelling a single component of male sweat alters levels of cortisol in women. *J Neurosci* 27(6):1261–1265.